

1
2
3 DOI: 10.1002/ adem.201500418
4

5 **Inner architecture of bonded splats under combined high pressure and shear**
6

7
8 *S. Khoddam*^{1*}, *T. Sapanathan*^{2,5}, *S. Zahiri*³, *P. D. Hodgson*¹, *A. Zarei-Hanzaki*⁴ and *R. Ibrahim*²
9

10 ¹*Institute for Frontier Materials (IFM), Deakin University, Geelong, VIC3216, Australia*

11 ²*Department of Mechanical Engineering, Monash University, VIC3800, Australia*

12 ³*CSIRO Materials Science and Engineering (CMSE), Victoria 3169, Australia*

13 ⁴*School of Metallurgy and Material Engineering, University of Tehran, Tehran, Iran*

14 ⁵*Laboratoire Roberval, UMR CNRS 7337, Université de Technologie de Compiègne, 60203*

15 *Compiègne, France*

16 ** Corresponding author Phone: +61 3 5227 1102, Fax: 03 5227 1103, E-mail:*

17 *shahin@deakin.edu.au*
18
19
20

21 **Abstract**

22 The inner architecture of material plays a seminal role in its overall properties. Micron size
23 commercial purity aluminium particles are deformed into an assembly of “interlocked splats” at room
24 temperature under a combination of high pressure and shear. This results in fabrication of highly
25 dense, strong and ductile samples. Dissections of the sample at different radii and planes are
26 examined to construct a “lookout map” featuring *splat shaped* deformed particles to study the
27 induced inner architecture. The structure comprises of splats of large “radial to axial aspect ratio”,
28 spread in parallel planes normal to the cylinder’s axis. Micro shear punch (MSP) tests are carried out
29 to characterize the heterogeneous strength properties and the radial distribution of material’s density.
30 A dimensional formulation is developed to interpret the MSP test data, taking into account some key
31 parameters of the structure. The consolidated samples show an excellent shear strength; stronger than
32 its solid counterpart and a pattern of radial strength distribution which is different with that of a
33 similar solid sample.
34
35
36
37
38
39
40
41
42
43
44
45
46
47
48
49
50

51 **Key words:** Metal forming and shaping; powder technology; deformation and fracture; inner
52 architecture
53
54
55
56
57
58
59
60
61

1
2
3 *Introduction*
4

5 Natural “Inner Architecture” (IA) in biological structures has inspired researchers to apply the natural
6 design principles into man-made materials^{[1][2][3][4]}. Particle-particle bonding, as the base for
7 fabrication of many products directly from powder, has potentials to produce products with artificial
8 inner architecture^{[5][6]}. A possible scenario is mechanical bonding of particles resulted by their
9 concurrent arranging, deforming and “grain refining”^{[7][8]} to enhance strength and ductility of the
10 product. The development of architected materials often requires new processes (e.g. ^[9]).
11
12
13
14
15
16
17
18
19

20 High Temperature Superconductive (HTSC) tapes are produced from brittle “Bismuth Strontium
21 Calcium Copper Oxide” using a “powder in tube” process ^[10]. Satisfactory performance of the tapes
22 depends on grain alignment. Eliminating the heat treatment improves the “weak links” which is a
23 major goal of researchers concerned with making HTSC tapes. A room temperature *particle bonding*
24 without metallurgical interaction at the interfaces can be a new paradigm for material design.
25
26
27
28
29

30 Eliminating heat treatment reduces carbon footprint and improves production rate for parts.
31

32 Combined shear and high pressures are commonly employed to produce bulk nano-structured
33 materials (e.g. equal channel angular pressing with additional extrusion step^[11] and a novel two step
34 High Pressure Torsion (HPT)^[12]). A review on this topic identifies the limitations on grain refinement
35 for single-phase and multi-phase materials using severe plastic deformations^[13]. Reducing the
36 processing requirements (e.g. a high pressure and processing time) is desirable and makes the
37 processes more practical.
38
39
40
41
42
43
44
45
46
47
48

49 We produced highly dense solid samples composed of *streamlined deformed particles*, hereafter
50 called “*splats*”, at the presence of shear and high pressure with a strong *particle bonding* at room
51 temperature using a Confined High Pressure Torsion (CHPT) processing. It requires low-moderate
52 processing (only 1.5 GPa pressure and 2 rotations), contrary to the conventional HPT processes
53 which require processing under 2.5-15 GPa with 5-60 rotations ^{[14][15][16][17][18][19]}. Moreover this
54
55
56
57
58
59
60
61

process minimizes the drawbacks in the conventional HPT process such as significant flash out of materials [20], effect of misalignment of anvils [20][21] and presence of dead zone [22][21].

To demonstrate the compliance of our processing with the proposed paradigm, some key parameters of its IA (excluding grain refinement in the particles) are discussed. These include particles' aspect ratio, compaction density, shear strength and their distribution. Effectiveness of the resulted IA is assessed by the arrangements of the processed particles and the excellent mechanical properties in the fabricated samples. The work also signifies the strength of the sample, as a function of chosen IA parameters. The optimum IA parameters have been studied analytically and experimentally.

A dimensional analysis is developed to understand the interaction of IA parameters in the sample.

Experimental results and discussion

Fabrication process and microstructure of the sample: Fig. 1 shows SEM image of aluminium powder particles (99.7% purity) and basics of Confined High Pressure Torsion (CHPT). The as received Al powder is ECKA Granules® 75s with bulk density of 1250 kgm^{-3} and average particle diameter of $28.0 \text{ }\mu\text{m}$. The samples with $r_o = 8\text{mm}$ and $t = 2\text{mm}$ were produced, applying 1.5GPa pressure and two rotations (Fig. 1).

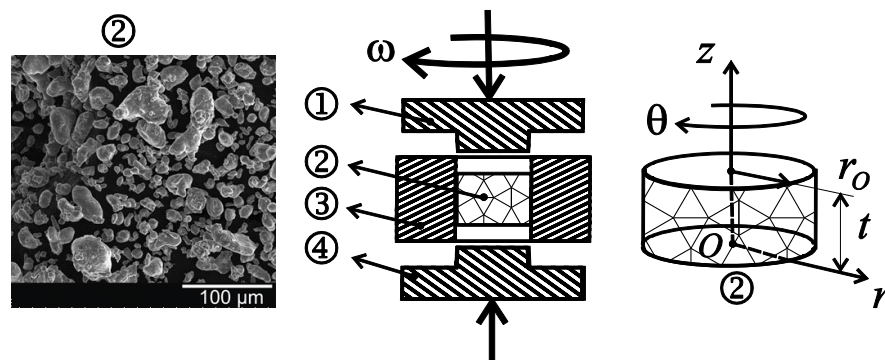


Fig. 1. Powder compaction using CHPT; left: SEM image of the Al particles before compaction, middle: 1 top punch (rotary), 2 CHPT sample, 3 constraining die and 4 lower punch (stationary), right: the coordinate system and dimensions.

1
2
3 A “lookout map”, a set of images showing the *splats’ boundaries* across different radii and
4
5 orientations, is shown in **Fig 2**. It shows distribution of splats’ shape in the sample in two orthogonal
6
7 planes along the radial and axial directions. Fig. 2-1 and 2 show the distribution, normal to z , along r
8
9 axis. Elongated splats in Fig. 2-2 near the sample’s periphery have a large aspect ratio of $l_\theta/l_r \gg 1$
10
11 (l_θ and l_r are splat length in θ and r directions respectively). Figs. 2-3 to 2-5 show the distributions,
12
13 normal to r , along r axis. Elongated splats in Fig. 6-5 near the periphery have a large aspect ratio of
14
15 $l_\theta/l_z \gg 1$ (l_z is splat length in z direction). Inset of Fig. 2-6, shows boundaries for a splat and its
16
17 inner substructure together. To explore a typical “triple-junction” at the interface of three splats,
18
19 careful preparation of the interface is necessary to keep the void intact. A Focused Ion Beam (FIB)
20
21 preparation and imaging was used here (Fig. 2-7) to minimize alteration of the gap/junction and the
22
23 boundaries by mechanical/ chemical preparations.
24
25
26
27
28
29
30
31
32
33
34
35
36
37
38
39
40
41
42
43
44
45
46
47
48
49
50
51
52
53
54
55
56
57
58
59
60
61
62
63
64
65

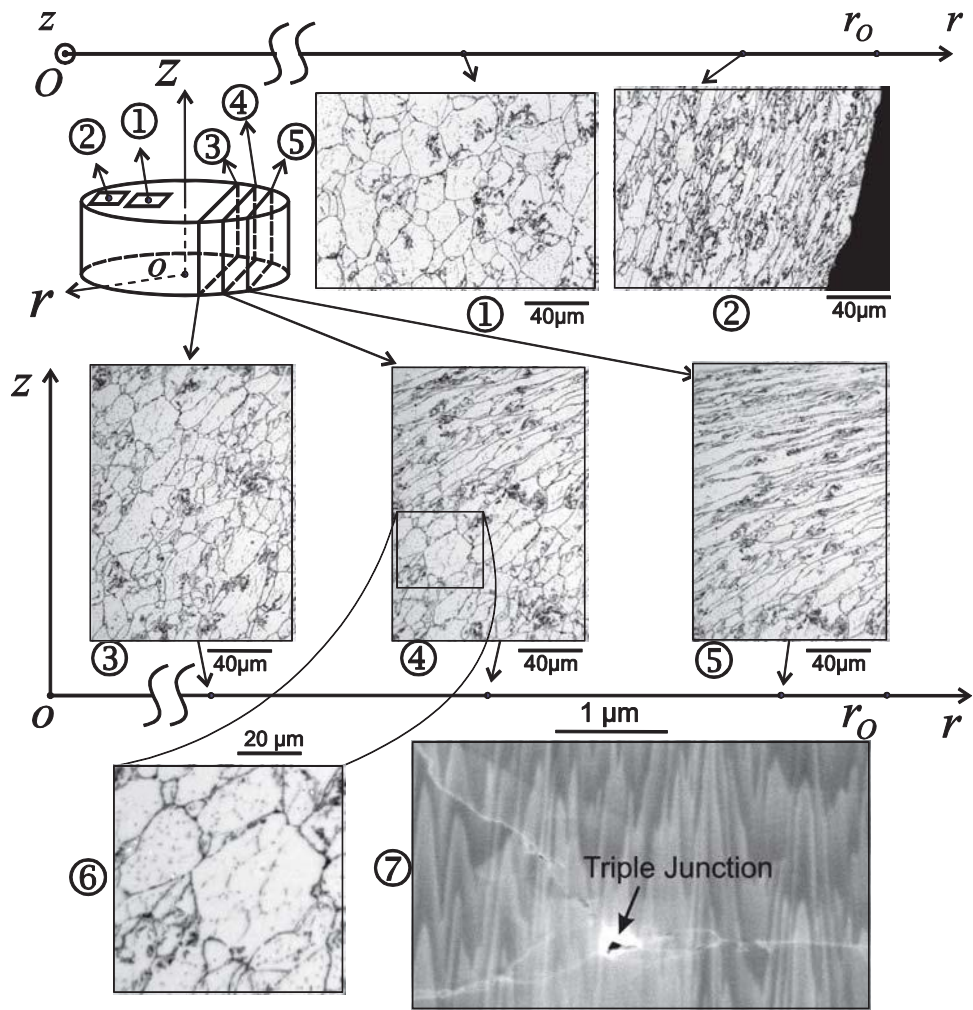


Fig. 2. The lookout map; Top left-location and orientation of the images in the sample. 1 and 2: optical micrographs near the centre and periphery, respectively (normal to z). 3, 4 and 5: optical micrographs near the centre (normal to r), middle and periphery of the sample, respectively. 6: an inset of 4. 7: a FIB dissection of a triple-junction.

Both “Splat boundaries” (shown in Fig. 2 as dark solid lines) and “grain structures” are key to study the IA of the sample as they are responsible for an effective interlocking and splat’s strength, respectively. Fig. 2-6 also shows substructures inside the corresponding splats of Fig. 2-4. To explore the nature of such sub-structures and the extent of grain refinement is beyond the scope of current work.

The process results in spreading and elongating *particles* by deformation and interlocking them together. As shown in Fig. 2, the splats’ “spreading and thinning” normal to z axis increases by

1
2
3 increasing their distance from the centre, r . Splats have random shape near the sample's centre and
4
5 elongate near the edges with their aspect ratio of $l_{\theta}/l_z \gg 1$ and $l_r/l_z \gg 1$. As a result, a good
6
7 mechanical interlocking can be expected. For a quantitative assessment of the property distribution in
8
9 the radial direction, the shearing strength behaviour, micro-hardness and density at different radii are
10
11 measured, analysed and explained next.

12
13
14
15 *Characterizing distribution of in situ mechanical properties of the sample:* For benchmarking of the
16
17 sample's strength and its distribution in the radial direction, three *sample types* were used: 1. CHPT
18
19 sample, 2. commercially pure Al (CP-Al) solid sample and 3. aluminum alloy Al5005-H34 solid
20
21 sample. Tests are performed at different radii to investigate the radial distribution of the samples'
22
23 shear strength, micro-hardness and density.
24
25

26
27 *Micro shear punch (MSP) test:* The fabricated samples are relatively small, the MSP test ^[23] is used
28
29 here as a "small specimen test" technique ^[24] to assess the sample's shear strength at localized regions.
30
31

32 **Fig. 3a** shows the MSP schematic and the positioning of the CHPT sample in the setup with five
33
34 sampling points of different radii; r_1, r_2, \dots and r_5 (H1, H2, \dots and H5, respectively- $0 \leq r_i \leq$
35
36 $6mm$) with a punch radius of $r_p = 1.5mm$. Fig. 3b shows a SEM image of a blanked out MSP's
37
38 piece. Typical "fracture" and "burnish" zones around the piece (shown as insets of 3c and d,
39
40 respectively) are visible; the latter comprises almost 40% of the total 2mm width which indicates a
41
42 ductile fracture. The MSP tests were also undertaken for the 2nd and 3rd sample types; for the
43
44 Al 5005-H34 sample, the 3rd type, tests were carried out at two different point T1 and T2 (Fig. 3e) to
45
46 confirm material's homogeneity and the test's repeatability. All of the tests were performed with a
47
48 strain rate of $\dot{\epsilon} = 0.01 \text{ s}^{-1}$. The results, compared with those of the CHPT sample (type1), are shown in
49
50 Fig. 3e.
51
52

53
54
55
56
57 *Density:* Densities of the MSPT's blanked pieces, ρ_i ($i = 1$ to 5), were measured (Fig. 3f). Central
58
59 part of the sample, $0 \leq r_i \leq 3.5mm$, had the highest density ratio (~98%) which dropped sharply to
60
61

1
2
3 90% outside the zone ($3.5 \leq r_i \leq 6.0$ mm). Void collapse, as a main mechanism for the compaction,
4
5 is easier in the central zone where the “radial rearrangement” is less restricted. A limited
6
7 rearrangement near the edges, where the particles could only rearrange inward, explains its lower
8
9 densification compared to that of the centre. Less porosity, increases density and decreases a non-
10
11 hydrostatic pressure status in the media which is a pre-requisite for particle’s super-plasticity. Very
12
13 few *triple-junctions* of $\leq 0.1\mu\text{m}$ in size (Fig.2-7) indicate a high compaction (density ratio), a good
14
15 mechanical interlocking and a high strength for the sample.
16
17
18
19
20
21
22
23
24
25
26
27
28
29
30
31
32
33
34
35
36
37
38
39
40
41
42
43
44
45
46
47
48
49
50
51
52
53
54
55
56
57
58
59
60
61
62
63
64
65

1
2
3
4
5
6
7
8
9
10
11
12
13
14
15
16
17
18
19
20
21
22
23
24
25
26
27
28
29
30
31
32
33
34
35
36
37
38
39
40
41
42
43
44
45
46
47
48
49
50
51
52
53
54
55
56
57
58
59
60
61
62
63
64
65

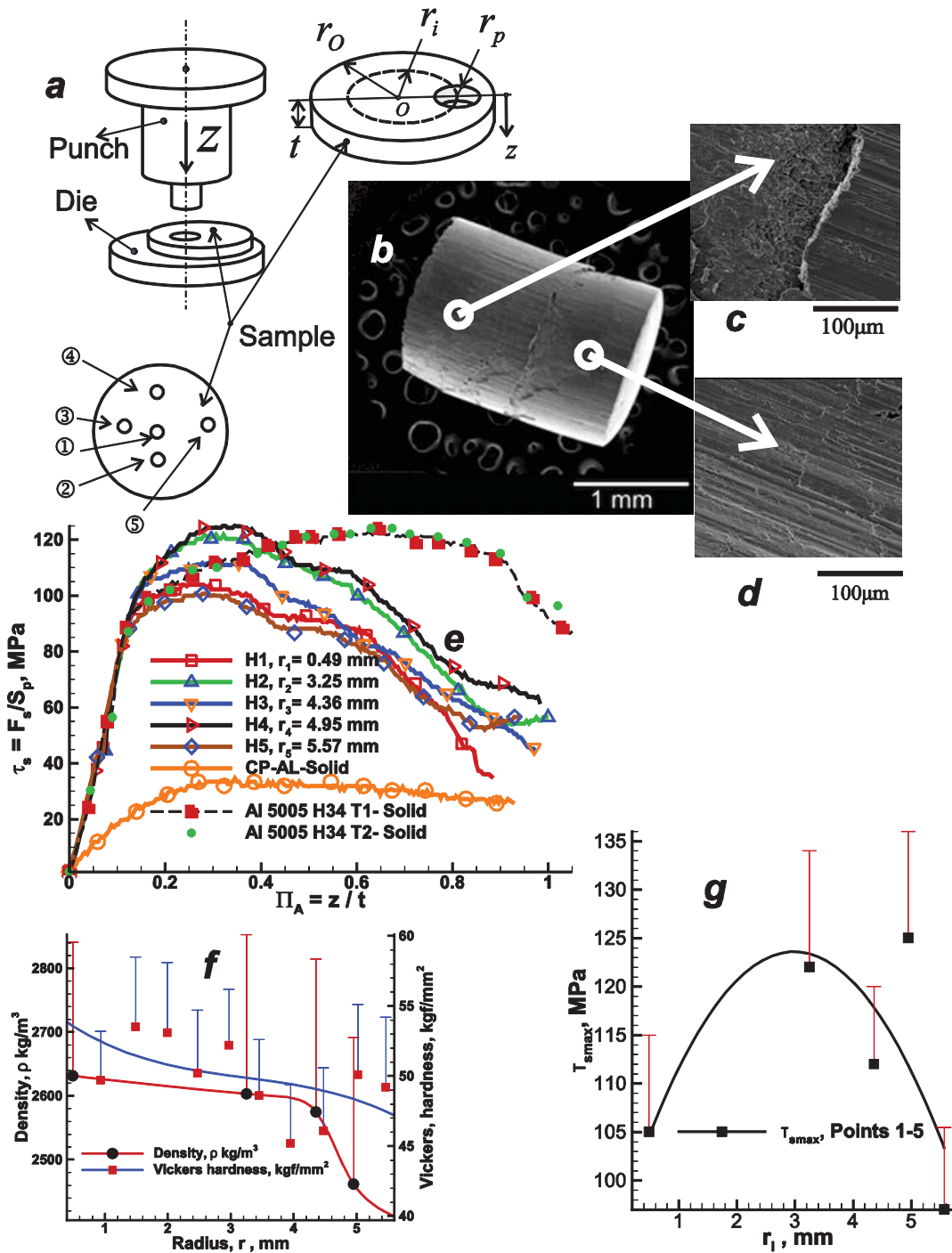


Fig. 3. a) Micro shear punch tests at five sampling points H1 to H5, b) a blanked piece, c) brittle fracture zone, d) ductile fracture zone, e) shearing strength at H1 to H5 for the 3 sample types, f) density and Vickers hardness in radial direction and g) maximum shearing stress vs. r_i at H1 to H5.

Micro hardness: Micro hardness across the samples' mid-planes along radial direction was measured using 10g load with 15 sec dwelling time using a Matsuzawa micro hardness tester MHT-1 according

1
2
3 to ASTM: E384 11e1 to prevent the variation in hardness distribution in top and bottom surfaces .The
4
5 results, shown in Fig. 3f, indicate that Vickers hardness drops moderately from its maximum
6
7 $\sim 53 \text{ kgf/mm}^2$ at the center to $\sim 47 \text{ kgf/mm}^2$ at the sample's edge. The average hardness of CP-Al
8
9 and Al5005-H34 samples was also measured to compare with the processed sample. The pure CP-Al
10
11 and Al5005-H34 samples was also measured to compare with the processed sample. The pure CP-Al
12
13 sample had an average hardness of 17.7 kgf/mm^2 which is significantly lower than that of the
14
15 processed sample. Also, the Al5005-H34 sample had an average hardness of 53.2 kgf/mm^2 which is
16
17 close to the highest hardness for the processed material (Fig. 3f).
18

19
20 A micro hardness measurement, with a small 10g load, is an indication of the surface strength instead
21
22 of specimen's overall strength across its thickness. Care must be taken when interpreting such
23
24 measurements due to the likely presence of pores in the vicinity of the indenter. The measurement is
25
26 also a point value which represents the surface strength immediately after the process. It is desirable
27
28 to have an understanding of the overall mechanical properties of the sample across its thickness and
29
30 to evaluate material's response under loading up to its failure. Given the small size of the sample, this
31
32 was achieved here using the MSP test which are complementary to the hardness data.
33
34

35
36 For all sampling points H1-5, the CHPT sample's shearing strength, represented by the MSP
37
38 response, is nearly "four times" higher than the solid CP-Al's strength and comparable with the Al
39
40 5005's strength. HPT processing of solid samples (e.g. [25]) produces a typical "radial gradient of
41
42 strength". This reduces with an increase in the number of revolutions while for two revolutions, the
43
44 gradient is significant. However according to Fig. 3e and 3 g, the CHPT sample's shearing strength
45
46 shows a different gradient. The response is not homogeneous and changes in radial direction. In the
47
48 specimen's central part, $0 \leq r_i \leq 5\text{mm}$, the shearing strength increases with radius (points 1 to 3 in
49
50 Fig. 3g). A further increase of radius, points 4 and 5, reduces the maximum shearing strength.
51
52

53
54 Despite some similarities between HPT and CHPT, their processed samples show different
55
56 heterogeneity patterns.
57
58

1
2
3 The CHPT sample's IA is an open ended topic with an extensive list of parameters that impact the
4
5 design. For example, the topic can be understood by studying the radial gradient of grain refinement
6
7 in the splats. Also, a key question is the role of splat's aspect ratio and orientation on mechanical
8
9 strength of the sample. The parameter sets considered here include: splat size, aspect ratio, density,
10
11 MSP strength behaviour and hardness. To gather a preliminary understanding of the sample's
12
13 performance, we develop a mathematical description for the MSP response taking into account the
14
15 parameters measured at different radii. We utilize these, in the next section, in a dimensional analysis
16
17 framework. Other aspects of IA are open for future works.
18
19
20

21
22 *Similarity theory applied to the MSP response:* Since the MSP response of the samples is governed
23
24 by several parameters, a model is developed, using the similarity theory (e.g. [26]), to understand the
25
26 interaction between them.
27
28

29 We define a parameter, λ_i , splat's representative aspect ratio at a sampling point i , as following:
30
31

$$\lambda_i = \frac{\bar{\lambda}_i}{\tilde{\lambda}} \quad (1)$$

32
33 Where $\bar{\lambda}_i$ is the average splat's aspect ratio in the punch's footprint and $\tilde{\lambda}$ is an optimum splat's
34
35 aspect ratio for which the processed material has its maximum shearing strength. Also, we designate
36
37 Vickers hardness at the punch's footprint for the i^{th} sampling point by H_i . It is assumed that MSP
38
39 force, F_s , mainly depends on effective strain rate $\dot{\epsilon}$, "density ρ_i at punch's footprint", "punch's
40
41 instantaneous stroke (penetration) z ", λ_i , H_i , "sample thickness t " and "the MSP's shearing area $S_p =$
42
43 $2\pi r_p t$ ":
44
45
46
47
48
49

$$F_s = F_s(\dot{\epsilon}, \rho_i, z, t, S_p, H_i, \lambda_i) \quad (2)$$

50
51 Using "Buckingham- Π theorem", five dimensionless parameters, $\Pi_A = z/t$, $\Pi_B = \dot{\epsilon}^2 t^2 \rho / H_i$, $\Pi_C =$
52
53 $F_s / (H_i t^2)$, $\Pi_D = S_p / t^2$ and $\Pi_E = \lambda_i$ are identified. A correlation function, f , is defined between the
54
55 parameters as:
56
57
58
59
60
61

$$\frac{F_s}{H_i t^2} = f\left(\frac{z}{t}, \frac{\dot{\epsilon}^2 t^2 \rho}{H_i}, \frac{S_p}{t^2}, \lambda_i\right) \quad (3)$$

To develop an expression for F_s as a function of radius r_i (Fig. 3e), we define a compound dimensionless parameter which is the product of four dimensionless parameters as following:

$$\Pi_B \cdot \Pi_C \cdot \Pi_D \cdot \Pi_E = \frac{\dot{\epsilon}^2 \lambda_i S_p \rho F_s}{H_i^2 t^2} \quad (4)$$

Two MSP tests at the two sampling points, r_1 and r_2 ($r_1 < r_2$), are considered here with identical values of $\dot{\epsilon}$, S_p and t . It can be shown that two compound parameters corresponding to the points are equal. Consequently, a ratio of F_s for the two tests can be expressed as:

$$\frac{(F_s)_{r_1}}{(F_s)_{r_2}} = \left(\frac{H_1}{H_2}\right)^2 \times \frac{\lambda_2}{\lambda_1} \times \frac{\rho_2}{\rho_1} \quad (r_1 < r_2) \quad (5)$$

A quadratic behaviour of F_s vs. r in Fig. 3g indicates that materials shearing strength is maximum at $r \approx 3.95$ mm. Given the unimodal (descending) behaviours of H and ρ vs. r (Fig. 3e) and Eq. 5, it can be concluded that λ_i should change quadratically with radius, r . If $\tilde{\lambda}_i$ is located at $r = \tilde{r}$, the conclusion may be restated as: for $0 < r < \tilde{r}$ an increase of λ_i increases materials' shearing strength and beyond this point ($\tilde{r} \leq r \leq r_o$) an increase of λ_i reduces the strength. Finding the exact location of \tilde{r} is complex as F_s represents the response of a relatively large footprint.

The CHPT produces considerable friction induced shear between the particles. This fabricates highly heterogeneous and interlocked “splats” and a strong bulk sample. Equation 3 and its special cases (e.g. Eq. 4) provide insight on how mechanical properties of the sample are correlated. Splat's aspect ratio, λ_i , may be considered as a parameter related to the interlocking of the splats which has a pronounced effect on the material's shearing strength.

Further works are needed to explore other aspects of the IA such as “grain structure changes” during the process and their impact on the final strength.

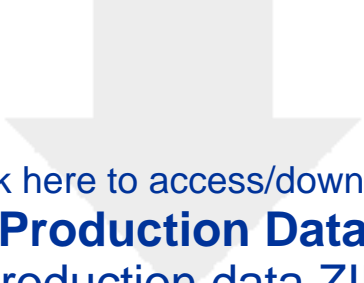
Conclusions

1
2
3 Strong and dense samples were fabricated using micron size Al particles processed by the CHPT at
4
5 room temperature under 1.5GPa pressure and two full revolutions. The splats' IA and their impact on
6
7 the sample's properties were explored. Lookout maps showed streamlined splats, in planes normal to
8
9 z axis and almost equiaxed in the sample's centre. Increasing their distance from the centre, splats
10
11 were elongated and thinned with their aspect ratios of $l_{\theta}/l_z \gg 1$ and $l_r/l_z \gg 1$ near the edges.
12
13 Formation of *very few triple-junctions* indicated a high densification with a maximum compaction
14
15 ratio of 98% near the centre of the sample. The CHPT sample revealed a ductile fracture during the
16
17 MSP tests at different radii. Also sample's density and hardness decreased monotonically along the
18
19 radial direction with their maximums at the centre and a sharp reduction of density near the
20
21 periphery. Conducting MSP tests for solid samples of CP-Al and Al-5005-H34 showed that the
22
23 CHPT sample was ~4 times stronger than the former, comparable with the later in shear and less
24
25 formable than the both solid samples. Heterogeneous distribution and aspect ratios of splats
26
27 contributed in their mechanical interlocking and the high strength of the CHPT sample evidenced by
28
29 the MSP results. A similarity theory was employed to correlate the IA parameters of the sample and
30
31 to interpret the strength results. It was concluded that there is a limit in improving shearing strength
32
33 of the processed material by increasing the splat's aspect ratio. Increasing the aspect ratio beyond this
34
35 limit, near the fabricated sample's periphery, reduces the sample's shearing strength.
36
37
38
39
40
41
42
43
44
45

46 **References:**

- 47
48 [1] O. Bouaziz, H. S. Kim, Y. Estrin, Adv. Eng. Mater. 2013, 15, 336.
49 [2] S. Deville, Adv. Eng. Mater. 2008, 10, 155.
50 [3] J. F. Mano, Adv. Eng. Mater. 2008, 10, 515.
51 [4] M. Kamperman, E. Kroner, A. Del Campo, R. M. McMeeking, E. Arzt, Adv. Eng. Mater. 2010, 12, 335.
52 [5] N. Travitzky, A. Bonet, B. Dermeik, T. Fey, I. Filbert-Demut, L. Schlier, T. Schlordt, P. Greil, Advanced
53 Engineering Materials 2014, 16, 729.
54 [6] Y. Beygelzimer, Y. Estrin, R. Kulagin, Adv. Eng. Mater. 2015, article in press, 1.
55 [7] W. Xu, X. Wu, T. Honma, S. P. Ringer, K. Xia, Acta Mater. 2009, 57, 4321.
56 [8] M. Kubota, X. Wu, W. Xu, K. Xia, Materials Science and Engineering: A 2010, 527, 6533.
57 [9] S. Khoddam, Y. Estrin, H. S. Kim, O. Bouaziz, Mater. Des. 2015, 85, 404.
58 [10] R. G. Abhilash Kumar, K. Vinod, R. P. Aloysius, U. Syamaprasad, Materials Letters 2006, 60, 3328.
59
60
61
62
63
64
65

- 1
2
3 [11] R. Z. Valiev, M. J. Zehetbauer, Y. Estrin, H. W. Höppel, Y. Ivanisenko, H. Hahn, G. Wilde, H. J. Roven, X.
4 Sauvage, T. G. Langdon, *Adv. Eng. Mater.* 2007, 9, 527.
5 [12] A. Bachmaier, M. Kerber, D. Setman, R. Pippan, *Acta Mater.* 2012, 60, 860.
6 [13] R. Pippan, F. Wetscher, M. Hafok, A. Vorhauer, I. Sabirov, *Adv. Eng. Mater.* 2006, 8, 1046.
7 [14] K. Kaneko, T. Hata, T. Tokunaga, Z. Horita, *Materials transactions* 2009, 50, 76.
8 [15] W. Botta Filho, J. Fogagnolo, C. Rodrigues, C. Kiminami, C. Bolfarini, A. Yavari, *Materials Science and*
9 *Engineering: A* 2004, 375, 936.
10 [16] A. Yavari, C. Rodrigues, C. Cardoso, R. Valiev, *Scripta Materialia* 2002, 46, 711.
11 [17] A. Bachmaier, R. Pippan, *Materials Science and Engineering: A* 2011, 528, 7589.
12 [18] Z. Lee, F. Zhou, R. Valiev, E. Lavernia, S. Nutt, *Scripta materialia* 2004, 51, 209.
13 [19] T. Tokunaga, K. Kaneko, K. Sato, Z. Horita, *Scripta Materialia* 2008, 58, 735.
14 [20] Y. Huang, M. Kawasaki, T. G. Langdon, *Advanced Engineering Materials* 2013, 15, 747.
15 [21] A. Hohenwarter, A. Bachmaier, B. Gludovatz, S. Scheriau, R. Pippan, *International Journal of Materials*
16 *Research* 2009, 100, 1653.
17 [22] D. J. Lee, E. Y. Yoon, L. J. Park, H. S. Kim, *Scripta Materialia* 2012, 67, 384.
18 [23] A. Farhoumand, S. Khoddam, P. D. Hodgson, *Modell. Simul. Mater. Sci. Eng.* 2012, 20.
19 [24] R. K. Guduru, K. A. Darling, R. Kishore, R. O. Scattergood, C. C. Koch, K. L. Murty, *Materials Science*
20 *and Engineering: A* 2005, 395, 307.
21 [25] G. Sakai, Z. Horita, T. G. Langdon, *Materials Science and Engineering: A* 2005, 393, 344.
22 [26] S. Khoddam, A. H. Shamdani, *J. Mater. Sci.* 2013, 48, 5579.
23
24
25
26
27
28
29
30
31
32
33
34
35
36
37
38
39
40
41
42
43
44
45
46
47
48
49
50
51
52
53
54
55
56
57
58
59
60
61
62
63
64
65



Click here to access/download
Production Data
production data.ZIP



Advanced Engineering Materials

Inner architecture of bonded splats under combined high pressure and shear

--Manuscript Draft--

Manuscript Number:	adem.201500418R2
Full Title:	Inner architecture of bonded splats under combined high pressure and shear
Article Type:	Communication
Section/Category:	
Keywords:	Metal forming and shaping; powder technology; deformation and fracture; inner architecture
Corresponding Author:	shahin Khoddam, PhD Institute for Frontier Materials AUSTRALIA
Additional Information:	
Question	Response
Please submit a plain text version of your cover letter here. If you are submitting a revision of your manuscript, please do not overwrite your original cover letter. There is an opportunity for you to provide your responses to the reviewers later; please do not add them here.	N/A
Corresponding Author Secondary Information:	
Corresponding Author's Institution:	Institute for Frontier Materials
Corresponding Author's Secondary Institution:	
First Author:	shahin Khoddam, PhD
First Author Secondary Information:	
Order of Authors:	shahin Khoddam, PhD Thaneshan Sapanathan, PhD Saden Zahiri, PhD Peter Hodgson, PhD Abbas Zarei-Hanzaki, PhD Raafat Ibrahim
Order of Authors Secondary Information:	